CrossMark

Ellipsometry of anisotropic graphene-like two-dimensional materials on transparent substrates

Peep Adamson[1]

Abstract

New possibilities for determining anisotropic properties of the dielectric constants of two-dimensional materials by ellipsometry are developed. Graphene-like 2D materials are considered within the framework of macroscopic electrodynamics as ultrathin absorbing anisotropic films where the optical axis is perpendicular to the film surface. The ellipsometric inversion problem is resolved analytically. The resulting inversion formulas are very fast because they allow you to directly calculate the complex anisotropic dielectric constants without the use of sophisticated regression analysis or iterative root-finding procedures. In particular, the method offers an interest in graphene and related 2D materials because the anisotropic properties of such materials have not been studied to date.

Keywords Ellipsometry · Graphene · Two-dimensional materials · Optical properties

1 Introduction

Graphene and related two-dimensional materials have gained most interesting due to their extraordinary properties (Novoselov et al. 2012; Li et al. 2017; Duong et al. 2017). Although the parameters of such materials have been thoroughly investigated, the problem of their anisotropic properties is still unresolved. At the same time, it is well known that the multi-layer graphene (highly oriented pyrolithic graphite) is anisotropic material with uniaxial anisotropy (the optical axis is perpendicular to the graphene sheets) (Jellison et al. 2007). Thus, it is reasonable to suppose that mono- and few-layer graphene are also anisotropic materials (Kravets et al. 2010; Song et al. 2018).

On the other hand, since a two-dimensional material is extremely thin, the effect its possible anisotropy on the measured quantities is small and, therefore, it is clear that the evaluation of anisotropic features of 2D materials requires a highly sensitive optical method. Two widely used high-sensitivity optical methods for studying the ultrathin surface layers are the surface differential reflectance (Lazzari et al. 2009; Zaglmayr et al. 2014; Adamson 2011) and ellipsometry (Tompkins and Irene 2005; Losurdo et al. 2009; Oates et al. 2011a; Garcia-Caurel et al. 2013; Gilliot 2017). The ability of differential

---

✉ Peep Adamson
peep.adamson@ut.ee

[1] Institute of Physics, University of Tartu, W. Ostwaldi 1, 50411 Tartu, Estonia

reflectance to determine the anisotropic properties of graphene-like 2D materials was recently addressed in Adamson (2017). But when talking about ellipsometric measurements, it should be noted that for optical modelling of graphene and graphene-like 2D materials, in most cases, the isotropic model has been used (Nelson et al. 2010; Wurstbauer et al. 2010; Weber et al. 2010; Nelson et al. 2012; Matkovic et al. 2013; Cheon et al. 2014; Ochoa-Martínez et al. 2015; Li et al. 2016). Moreover, some authors argue that the error of the ellipsometers used by them in measuring ellipsometric angles Ψ and Δ is greater than the change in these ellipsometric angles caused by the anisotropy of the 2D material compared to the isotropic material and therefore the determination of anisotropy is not possible (Song et al. 2018; Nelson et al. 2012). Nevertheless, nowadays the properly aligned ellipsometer with high quality optics is capable of precision of about a few hundredths of a degree in Ψ and Δ (Losurdo et al. 2009). Although the contribution of the anisotropy of dielectric constants of 2D materials to the ellipsometric angles is indeed very small, the given measurement accuracy is also quite high and therefore the question remains whether there really is not any way to determine the anisotropic dielectric constants of 2D materials on the basis of ellipsometry.

The aim of this work is to analyze this issue in substance. Firstly, we consider the effect of anisotropy to the ellipsometric angles depending on the thickness d and wavelength λ (more precisely, on the ratio d/λ) and also on the strength of anisotropy of 2D materials. In other words, the question is how much the introduction of anisotropy changes the value of ellipsometric angles Ψ and Δ compared to isotropic 2D materials and when this change is greater than the measurement error in Ψ and Δ.

Secondly, we will analyze how it is possible to identify unknown parameters of anisotropy of 2D materials. We show that the determination of all anisotropic dielectric constants can be simply carried out by the measurements of two ellipsometric angles for two different transparent substrate materials. But if we assume that in the first approximation, the ordinary refractive index can be considered equal to the refractive index obtained from the isotropic model, the extraordinary refractive index of 2D materials can be determined only on the basis of ellipsometric angle Δ for single substrate material.

It should be pointed out that, in general, an unknown parameter is also the thickness of 2D materials. However, with a view to graphene-like 2D materials, it can be said that generally the thickness of their monolayers is well known and there are several methods that allow you to determine the number of layers in a few layer sheet of such materials (Ferrari 2007; Tan et al. 2012; Lui et al. 2012; Wang et al. 2012; Shearer et al. 2016). Therefore, in this work it has been assumed that the thickness of the 2D material is known in advance.

In addition to the above, it is also important to note that there is another interesting group of anisotropic 2D materials, namely, nanoparticle films (Bedeaux and Vlieger 2001; Oates et al. 2011b; Gwo et al. 2016). Using an effective medium theory (Humlicek 2013; Toudert et al. 2012) which approximates a nanocomposite film as a homogeneous medium (through the second average) we can describe the response of the nanoparticle layer by effective dielectric function as in the case of graphene-like 2D materials. This approach also opens up new interesting opportunities for optical diagnostics of anisotropic ultrathin nanoparticle layers because one can obtain the macroscopic polarization (dielectric function) as a function of the factors, which are linked to such parameters of nanoparticles as their shape, orientation, and size (Battie et al. 2016, 2017).

2 Method

We will consider 2D materials phenomenologically within the framework of macroscopic electrodynamics as absorbing ultrathin films with uniaxial anisotropy, where the optical axis is perpendicular to the film surface. The ordinary dielectric constant $\varepsilon_o = \varepsilon'_o + i\varepsilon''_o = n_o^2 = (n'_o + in''_o)^2$ and the extraordinary dielectric constant $\varepsilon_e = \varepsilon'_e + i\varepsilon''_e = n_e^2 = (n'_e + in''_e)^2$ are complex quantities. The incident light in a transparent ambient medium with dielectric constant $\varepsilon_a = n_a^2$ makes an angle φ_a with the substrate normal and the substrate is a semi-infinite isotropic and transparent material with real dielectric constant $\varepsilon_s = n_s^2$. Note that since in practice the thickness of a real substrate, of course, is not infinite, but final, then the light reflected from the back surface of the substrate must be suppressed. This is usually done by roughening the back surface or using a wedge substrate.

The analysis is based on the electromagnetic 4×4 matrix theory for anisotropic layered media with complex dielectric constants (Azzam and Bashara 1977; Yeh 2005). It is, however, appropriate to mention that, if the optical axis is perpendicular to the surface of the film, the reflection matrix (Jones matrix) is diagonal (i.e., $r_{ps} = r_{sp} = 0$) and general formulas for the amplitude reflection coefficients r_{pp} and r_{ss} can also be obtained from a simple model based on geometrical optics (Fujiwara 2007). However, strictly speaking, geometric optics is not applicable, if $d \leq \lambda$, although the formulas obtained for r_{pp} and r_{ss} remain formally valid for this simple asymmetry. Only an analysis on the basis of general electromagnetic theory proves this fact.

Within the framework of the long-wavelength limit (the film thickness d is much less than an optical wavelength λ) we obtain in the first order with respect to the small parameter d/λ the following expressions for the differential ellipsometric angles (in radians) if $\varphi_a \neq \varphi_B = \arctan(n_s/n_a)$:

$$\delta\Psi = \Psi - \Psi_0 = \sin 2\Psi_0 \; F(\varphi_a, \varepsilon_a, \varepsilon_s) \, (\varepsilon_a \varepsilon_s \, \varepsilon''_e |\varepsilon_e|^{-2} - \varepsilon''_o) \, \frac{d}{\lambda}, \tag{1}$$

$$\delta\Delta = \Delta - \Delta_0 = 2F(\varphi_a, \varepsilon_a, \varepsilon_s) \, (\varepsilon'_o + \varepsilon_a \varepsilon_s \, \varepsilon'_e |\varepsilon_e|^{-2} - \varepsilon_a - \varepsilon_s) \, \frac{d}{\lambda}, \tag{2}$$

$$F(\varphi_a, \varepsilon_a, \varepsilon_s) = \frac{2 \, \pi \, n_a \cos \varphi_a \sin^2 \varphi_a}{(\varepsilon_a \cos^2 \varphi_s - \varepsilon_s \, \cos^2 \varphi_a)}, \tag{3}$$

where $|\varepsilon_e|^2 = (\varepsilon'_e)^2 + (\varepsilon''_e)^2$, φ_s is the angle of refraction ($\cos^2 \varphi_s = 1 - \varepsilon_a \varepsilon_s^{-1} \sin^2 \varphi_a$), Δ and Ψ are the ellipsometric angles of a tri-layer (ambient-film-substrate) structure, Ψ_0 and Δ_0 are the ellipsometric angles of the bare substrate ($d = 0$), i.e., of the two-layer (ambient-substrate) system. Note that we can take $\Delta_0 = 0$ for the transparent substrates (of course, one should keep in mind that at the Brewster angle Δ_0 changes by $\pi/2$).

The accuracy of the first-order approximate Eqs. (1) and (2) for a given wavelength depends primarily on the film thickness. Comparison between the calculations that have been made on the basis of rigorous ellipsometric theory and by approximate Eqs. (1) and (2) shows that the accuracy of such formulas is good if $d/\lambda \leq 10^{-3}$ (Fig. 1). The condition $d/\lambda \leq 10^{-3}$ is always satisfied for 2D materials in the infrared spectral region. In the visible spectral region the accuracy of the first-order Eqs. (1) and (2) depends heavily on the thickness d and generally is no longer good. For example, for three-layer graphene ($d \approx 1$ nm) the errors of $\delta\Psi$ and $\delta\Delta$ are approximately 6.1% and 3.6%, respectively, if $\lambda = 500$ nm,
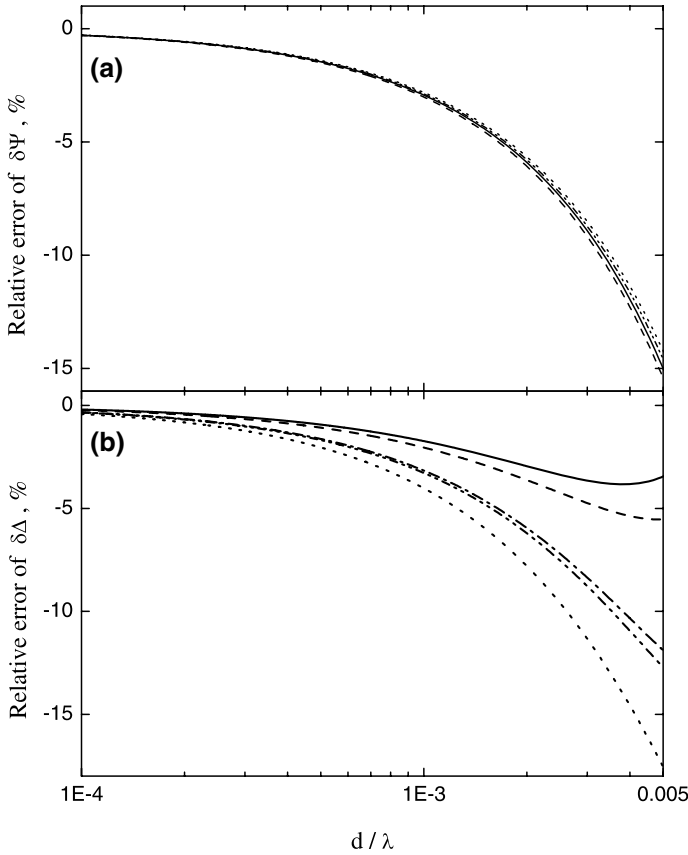
Fig. 1 Relative errors **a** of $\delta\Psi$ and **b** of $\delta\Delta$ as functions of d/λ for anisotropic layers with $n_o = 2.7 + i\,1.4$ and $n_e = 1.5$ (solid curves), $1.5 + i\,0.2$ (dashed curves), 2.0 (dash-dotted curve), $2.0 + i\,0.2$ (dash-dot-dotted curves), and 2.5 (dotted curves) at $n_s = 1.5$ and $\varphi_a = 70°$

$\varphi_a = 70°$, $n_o = 2.7 + i\,1.4$, $n_e = 1.5 + i\,0.2$, and $n_s = 1.5$. Note that the ambient refractive index $n_a = 1$ in all Figs. 1, 2, 3, 4, 5, 6, 7, 8, 9, 10, 11, 12 and 13.

Of course, the accuracy of Eqs. (1) and (2) also depends on the dielectric constants of the materials. If the dependence on the refractive index of 2D materials is not very noticeable (Fig. 1), then for the substrate material, two moments must be taken into account. First of all, Eqs. (1) and (2) are not applicable at the Brewster angle $\varphi_B = \arctan(n_s/n_a)$, i.e., the angle of incidence φ_a must satisfy the condition $\varphi_a < \varphi_B$ or $\varphi_a > \varphi_B$ (Fig. 2). Second, as follows from Eqs. (1) and (2), $\delta\Psi$ becomes zero if

$$n_s = [\,\varepsilon_o''/\varepsilon_e''\,]^{1/2}|\varepsilon_e|/n_a, \tag{4}$$

and $\delta\Delta$ becomes zero if

$$n_s = [\,(\varepsilon_o' - \varepsilon_a)\,(1 - \varepsilon_a\varepsilon_e'|\varepsilon_e|^{-2})^{-1}\,]^{1/2}. \tag{5}$$

For example, if $n_a = 1$, $n_o = 2.7 + i\,1.4$, and $n_e = 1.5 + i\,0.5$, then $\delta\Delta \approx 0$ at $n_s = 2.52$ (see also Fig. 2b) and $\delta\Psi \approx 0$ at $n_s = 5.61$, but if $n_a = 1$, $n_o = 2 + i$, and $n_e = 1.5 + i$,
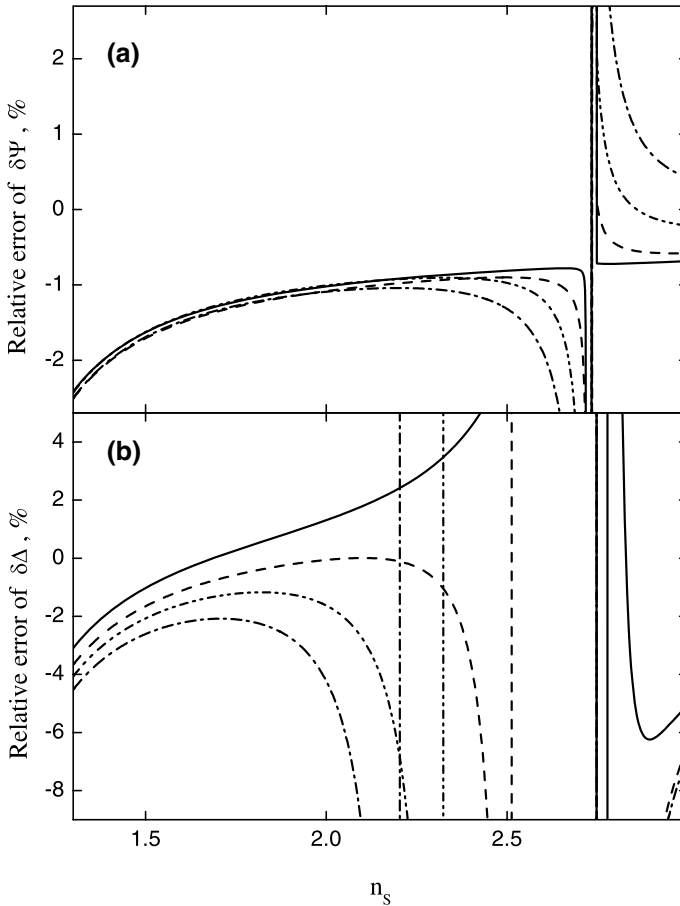
Fig. 2 Relative errors **a** of $\delta\Psi$ and **b** of $\delta\Delta$ as functions of n_s for anisotropic layers with $n_o = 2.7 + i\,1.4$ and $n_e = 1.5$ (solid curves), $1.5 + i\,0.5$ (dashed curves), $1.5 + i\,1.0$ (dash-dotted curves), and $2.0 + i\,0.5$ (dash-dot-dotted curves) at $d/\lambda = 5.583 \cdot 10^{-4}$ and $\varphi_a = 70°$

then $\delta\Psi \approx 0$ at $n_s = 2.75$. Note that in this paper in numerical estimates we often use for n_o the values, measured for the graphene refractive index n according to the isotropic model. But, generally, we use different values for n_o because there is considerable disagreement among the published values for n (Cheon et al. 2014). For n_e we also apply the different values, including those that are measured for graphite (Jellison et al. 2007; Song et al. 2018).

It is clear that around the zero points (4) and (5) first-order formulas do not work (Fig. 2b) because in this case it is not enough to take into account in a power series in the small parameter d/λ only the terms with first powers of d/λ.

In relation to the accuracy of approximate formulas, it is also important to note that it strongly depends on the angle of incidence φ_a, especially in the case of Eq. (2), the error of which is smaller for large incidence angles, for example, in the vicinity of 70° (Fig. 3).

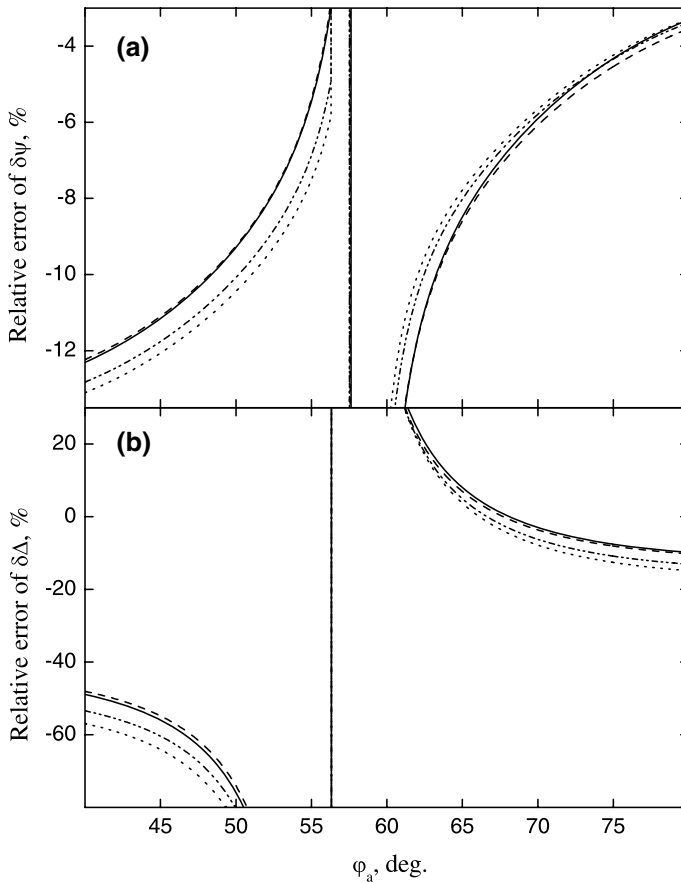**Fig. 3** Relative errors **a** of $\delta\Psi$ and **b** of $\delta\Delta$ as functions of φ_a for different anisotropic layers at $d/\lambda = 2 \cdot 10^{-3}$. The other parameters are the same as in Fig. 1

3 Results and discussion

The above analytic Eqs. (1) and (2) are of interest not only because they allow you to simply calculate the values of the ellipsometric angles $\delta\Psi$ and $\delta\Delta$, but above all because it is easy to solve the inversion problem on their basis, i.e., to determine the values of the dielectric constants of 2D materials by measuring the quantities $\delta\Psi$ and $\delta\Delta$.

Let us look at when and how it can be done on the basis of these relationships. The first question that arises immediately—what is at all an anisotropic effect on ellipsometric angles in the case of very small d/λ values where approximate formulas are applicable. The problem can also be formulated differently: what should be the accuracy of measuring ellipsometric angles in order to distinguish an anisotropic film from an isotropic. Nowadays it is safe to assume that properly aligned ellipsometer with high-quality optics is capable of precision of about $0.01°$–$0.02°$ in ellipsometric angles (Losurdo et al. 2009). Exact calculations, not based on the approximate Eqs. (1) and (2), show that ellipsometric angles $\delta\Psi$ and $\delta\Delta$ are measurable if $d/\lambda \geq 10^{-4}$ (Fig. 4). However, measurement of $\delta\Psi$ differences caused by anisotropy with this measurement error is not possible if $d/\lambda \leq 10^{-3}$. At the same time, ellipsometric angle $\delta\Delta$
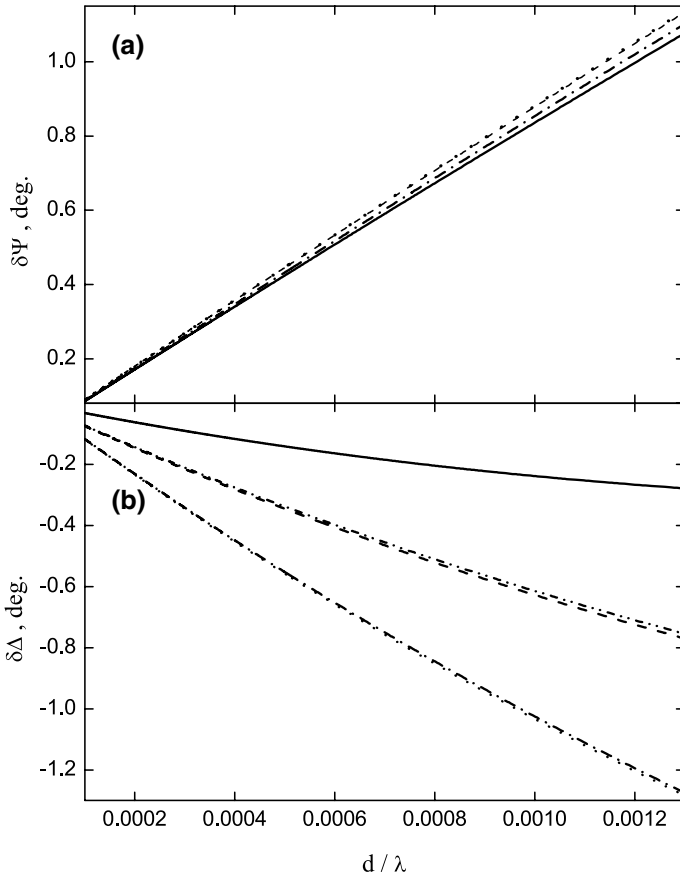
Fig. 4 Ellipsometric angles **a** $\delta\Psi$ and **b** $\delta\Delta$ as functions of d/λ for an isotropic layer with $n_o \equiv n_e = 2.7 + i\ 1.4$ (solid curves) and for different anisotropic layers with $n_o = 2.7 + i\ 1.4$ and $n_e = 1.5$ (dotted curves), $1.5 + i\ 0.1$ (dash-dotted curves), 2.0 (dashed curves), and $2.0 + i\ 0.2$ (dash-dot-dotted curves) at $n_s = 2.0$ and $\varphi_a = 55°$

is sufficiently sensitive to the real part of the extraordinary refractive index n_e if $d/\lambda \leq 10^{-3}$ but measuring the effects of small imaginary parts of n_e is also not possible (Fig. 4b).

In order to obtain a slightly more accurate picture of the anisotropic effect on the values of $\delta\Psi$ and $\delta\Delta$ (i.e., what are the differences $\delta\Psi - \delta\Psi_S$ and $\delta\Delta - \delta\Delta_S$, where $\delta\Psi_S$ and $\delta\Delta_S$ are the ellipsometric angles corresponding to the isotropic case $n_o = n_e$) we use Eqs. (1) and (2). Since in particular we are interested in the anisotropic characteristics of graphene, we focus on them. The theoretical analysis (Klintenberg et al. 2009) shows that for monolayer graphene $\varepsilon_e'' = n_e'' = 0$ and for few-layer graphene the values of imaginary part of ε_e are very small, therefore, for few-layer graphene in the first approximation we can also take $\varepsilon_e'' \approx 0$. In this case, we get from Eqs. (1) and (2) that

$$\delta\Psi - \delta\Psi_S \approx -\sin 2\Psi_0\ 2F(\varphi_a, \varepsilon_a, \varepsilon_s)\ \varepsilon_a \varepsilon_s \frac{n_o' n_o''}{(n_o'^2 + n_o''^2)^2}\ \frac{d}{\lambda}, \tag{6}$$
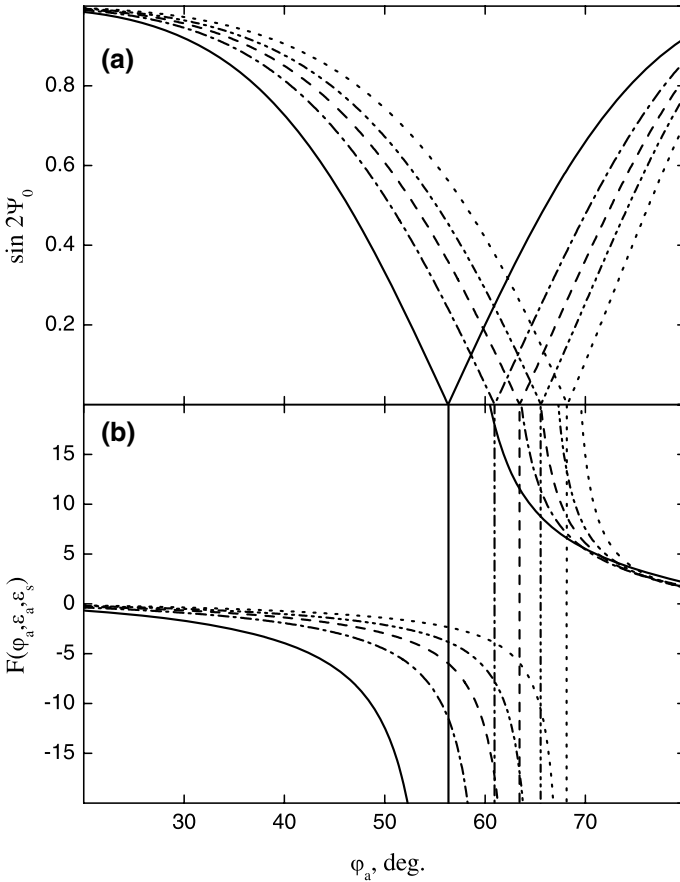
Fig. 5 **a** $\sin 2\Psi_0$ and **b** $F(\varphi_a, \varepsilon_a, \varepsilon_s)$ as functions of φ_a for different substrates with $n_s = 1.5$ (solid curves), 1.8 (dash-dotted curves), 2.0 (dashed curves), 2.2 (dash-dot-dotted curves), and 2.5 (dotted curves)

$$\delta\Delta - \delta\Delta_S \approx 2F(\varphi_a, \varepsilon_a, \varepsilon_s) \, \varepsilon_a\varepsilon_s \left(\frac{1}{n_e'^2} - \frac{(n_o'^2 - n_o''^2)}{(n_o'^2 + n_o''^2)^2} \right) \frac{d}{\lambda}. \tag{7}$$

Using the calculated values of $\sin 2\Psi_0$ and $F(\varphi_a, \varepsilon_a, \varepsilon_s)$ (Fig. 5), it is easy to evaluate changes in the ellipsometric parameters $\delta\Psi$ and $\delta\Delta$ caused by anisotropy. For example, taking $n_a = 1$, $n_s = 1.5$, $n_o = 2.7 + i1.4$, $n_e = 1.5$, and $\varphi_a = 65°$ we get that $\delta\Psi - \delta\Psi_S \approx -48°\,(d/\lambda)$ and $\delta\Delta - \delta\Delta_S \approx 920°\,(d/\lambda)$ or taking $n_s = 2.5$ and leaving the other parameters the same we get that $\delta\Psi - \delta\Psi_S \approx 50°\,(d/\lambda)$ and $\delta\Delta - \delta\Delta_S \approx -2410°\,(d/\lambda)$. In the visible spectral region, for graphene $d/\lambda < 10^{-3}$, so $\delta\Psi - \delta\Psi_S < 0.05°$, and measurement with even the best ellipsometers (expected measurement error $0.01° - 0.02°$) is not possible. But for a three-layer graphene $d/\lambda \approx 2.7 \cdot 10^{-3}$ at $\lambda = 500$ nm and $\delta\Psi - \delta\Psi_S \approx 0.1°$, and measuring such a difference is already possible, albeit with a big error.

The anisotropic effect, of course, also depends on the refractive index of the 2D material. However, it is interesting to note that in the case of graphene ($n_e'' = 0$), the effect of
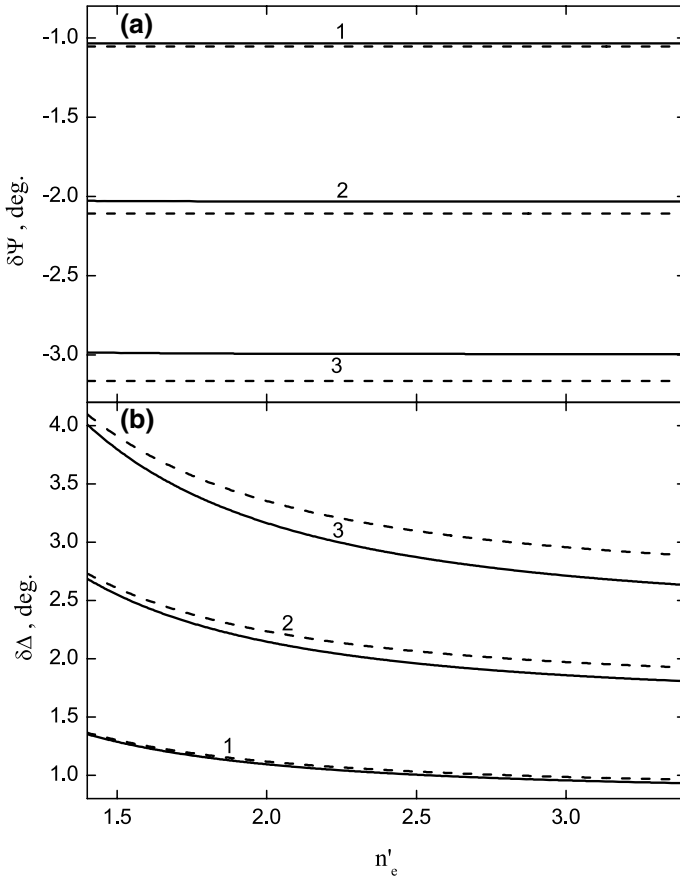
Fig. 6 Ellipsometric angles **a** $\delta\Psi$ and **b** $\delta\Delta$ as functions of n'_e for anisotropic monographene (1), bilayer graphene (2), and 3-layer graphene (3) with thicknesses $d = 0.335$ nm, $d = 2 \times 0.335$ nm, and $d = 3 \times 0.335$ nm, respectively, if $n_o = 2.7 + i\,1.4$, $n''_e = 0$, $\lambda = 500$ nm, $n_s = 1.5$, and $\varphi_a = 70°$. Dashed curves are calculated by the approximate Eqs. (1) and (2), solid curves by exact ellipsometric equations. Preceding numbers in parentheses are curve labels

the anisotropy on the ellipsometric angle $\delta\Psi$, i.e., the value of $\delta\Psi - \delta\Psi_S$, does not depend on the value of the extraordinary refractive index (n'_e) in the first approximation (see formula (6)). This fact is well illustrated by Fig. 6, which shows the dependencies of the ellipsometric angles $\delta\Psi$ and $\delta\Delta$ on the parameter n'_e for monolayer, bi-layer, and 3-layer graphene (this is also illustrated in Fig. 4a, where dotted and dashed curves practically merge together). Therefore, for graphene ($n''_e = 0$), the quantiy $\delta\Psi - \delta\Psi_S$ depends only on the ordinary refractive index n_o. For example, taking $n_a = 1$, $n_s = 1.5$, and $\varphi_a = 65°$ we get that $\delta\Psi - \delta\Psi_S \approx -87°\,(d/\lambda)$ for $n_o = 2 + i$ and $\delta\Psi - \delta\Psi_S \approx -39°\,(d/\lambda)$ for $n_o = 3 + i\,2$. At the same time, $\delta\Delta - \delta\Delta_S$ depends not only on the ordinary refractive index n_o, but also on the extraordinary refractive index $n_e = n'_e$ (Eq. (7)).

It must be pointed out, however, that the values of the anisotropy constants taken in the calculations are the same for graphenes with different number of layers, i.e., the values of n_o and n_e do not depend on the thickness of the graphene sheet. Of course, the question arises as to whether and to what extent the optical constants of the graphene sheet
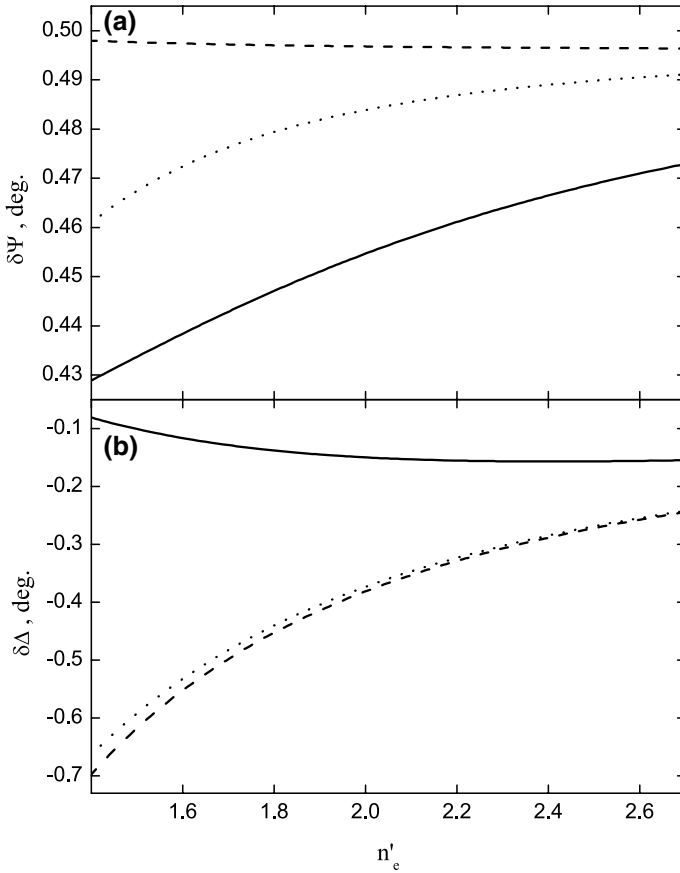
Fig. 7 Ellipsometric angles **a** $\delta\Psi$ and **b** $\delta\Delta$ as functions of n'_e for anisotropic layers with $n_o = 2.7 + i\,1.4$ and $n''_e = 1.4$ (solid curves), 0.2 (dotted curves), and 0 (dashed curves) at $d/\lambda = 5.583 \times 10^{-4}$, $n_s = 2.0$, and $\varphi_a = 55°$

depend on the number of layers in it. As there is no experimental data on the anisotropic dielectric constants of mono- and few-layer graphene, only theoretical works can be relied upon. Calculations show (Klintenberg et al. 2009) that anisotropic dielectric constants are quite independent of the number of graphene layers (the modification due to an increase in the number of layers is within a few per cent). The results are close to graphite, for which there are also experimental measurements (Jellison et al. 2007), which quite well coincide with theoretical calculations (Klintenberg et al. 2009) (note that the values of the single-layer graphene dielectric constant obtained on the basis of an isotropic model also fall in the first approximation with those of a few-layer graphene (Isic et al. 2011)). Physically, this is well understood, since dielectric constants are dominated by the electronic response and the energy scale at which the monographene and multilayer graphene band structures differ is determined by the energy of the interlayer coupling which is only a few hundreds of millielectronvolts (Min and MacDonald 2009). This is also the reason why we use the values of anisotropic dielectric constants measured for graphite in our computer simulations for graphene. It should be noted that, from the anisotropic point of view, graphenes

Fig. 8 Relative error of n'_e determined by Eq. (8) as a function of λ for anisotropic monographene ($n''_e = 0$) with $d = 0.335$ nm, $n_o = 2.7 + i\ 1.4$, and $n'_e = 1.5$. Instrumental error $v_\Delta = 0$ (solid curve), 1% (dashed curve), 2% (dotted curve), -1% (dash-dotted curve), and -2% (dash-dotdotted curve) at $n_s = 1.5$ and $\varphi_a = 68°$
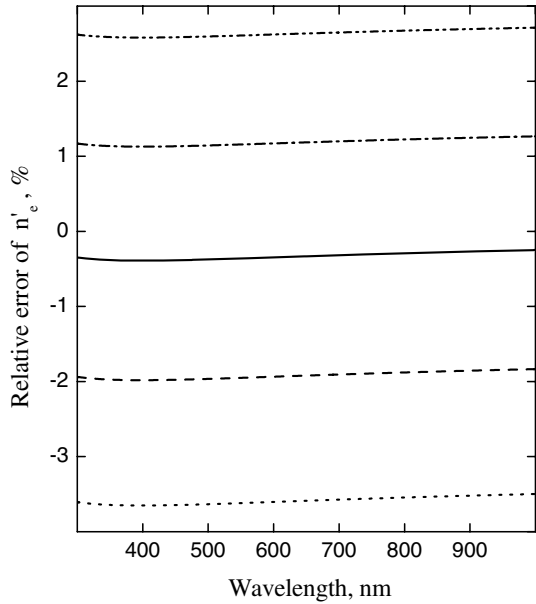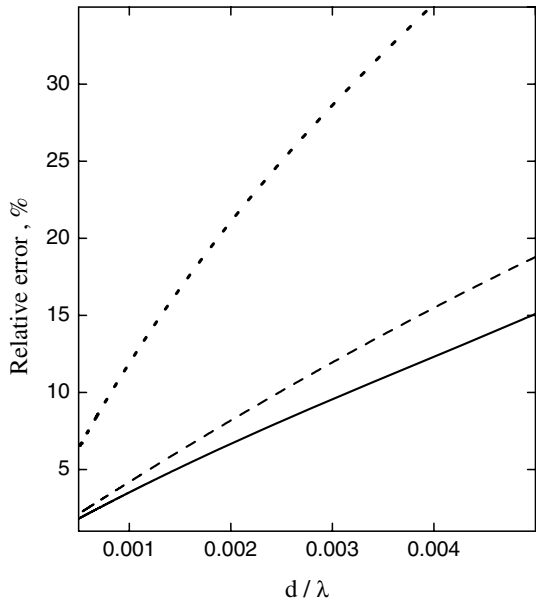

Fig. 9 Relative errors of ε'_o (solid curve), ε''_o (dashed curve), and ε'_e (dotted curve) determined by Eqs. (9), (10), and (11), respectively, as functions of d/λ for an anisotropic layer with $n_o = 2.7 + i\ 1.4$ and $n_e = 1.5$ at $n_s^{(1)} = 1.5$, $n_s^{(2)} = 2.0$, $\varphi_a = 70°$, and $v_\Delta = v_\Psi = 0$

are interesting materials, since the difference between n_o and n_e is quite large compared to conventional anisotropic materials.

In summary, the effect of anisotropy on the ellipsometric angle $\delta\Psi$ is considerably weaker than on the angle $\delta\Delta$. If $d < 1$ nm, then measuring $\delta\Psi - \delta\Psi_S$ is not practically
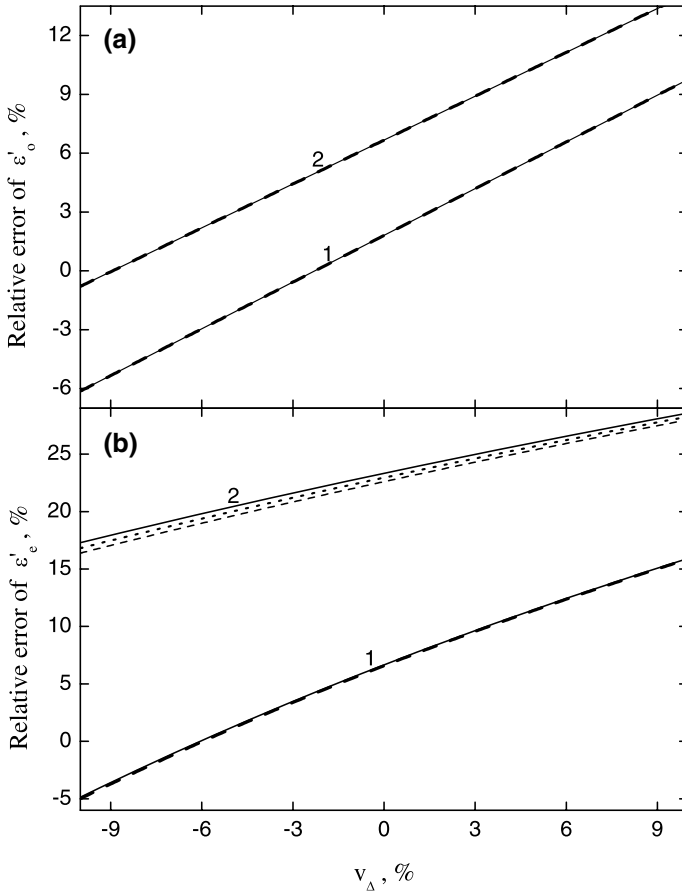
Fig. 10 Relative errors **a** of ε'_o and **b** of ε'_e determined by Eqs. (9) and (11), respectively, as functions of v_Δ at $v_\Psi = 0$ (dotted curve), 10% (dashed curves), and -10% (solid curves), $d/\lambda = 5 \times 10^{-4}$ (1) and 2×10^{-3} (2), $n_o = 2.7 + i\,1.4$, $n_e = 1.5$, $n_s^{(1)} = 1.5$, $n_s^{(2)} = 2.0$, and $\varphi_a = 70°$. Preceding numbers in parentheses are curve labels

possible. At the same time, $\delta\Delta - \delta\Delta_S$ measurement is well implemented in the visible spectral region. This is also illustrated by numerical calculations based on exact ellipsometric formulas (Fig. 7). In this figure it is clearly seen that the changes in the ellipsometric angle $\delta\Psi$ caused by anisotropy are in the order of a few hundredths of degrees, while corresponding to $\delta\Delta$ changes are in the order of a few tenths of degrees (the values for the isotropic case are located on solid curves at $n'_e = 2.7$).

Since $\delta\Delta$ is a well measurable quantity for monographene ($\varepsilon''_e = 0$), assuming that in the first approximation $n_o = n'_o + in''_o$ can be taken to be equal to the graphene refractive index n measured in accordance with the isotropic model, we can simply evaluate the value of ε'_e only by measuring $\delta\Delta$. Namely, from Eq. (2) it follows that

$$\varepsilon'_e = n'^2_e = \frac{\varepsilon_a \varepsilon_s}{(\delta\Delta/2F(\varphi_a, \varepsilon_a, \varepsilon_s))(\lambda/d) - \varepsilon'_o + \varepsilon_s + \varepsilon_a}. \tag{8}$$

Fig. 11 Relative error of ε_o'' determined by Eq. (10) as a function of v_ψ at $d/\lambda = 5 \times 10^{-4}$ (1), 1×10^{-3} (2), 2×10^{-3} (3), and 4×10^{-3} (4), $n_o = 2.7 + i\ 1.4$, $n_e = 1.5$, $n_s^{(1)} = 1.5$, $n_s^{(2)} = 2.0$, and $\varphi_a = 70°$. Preceding numbers in parentheses are curve labels
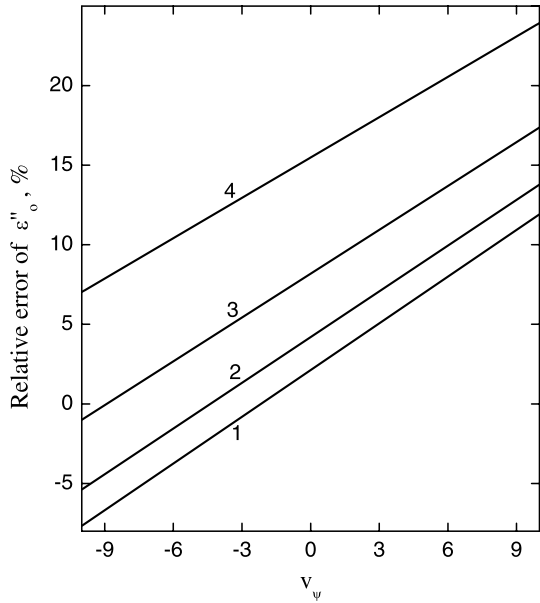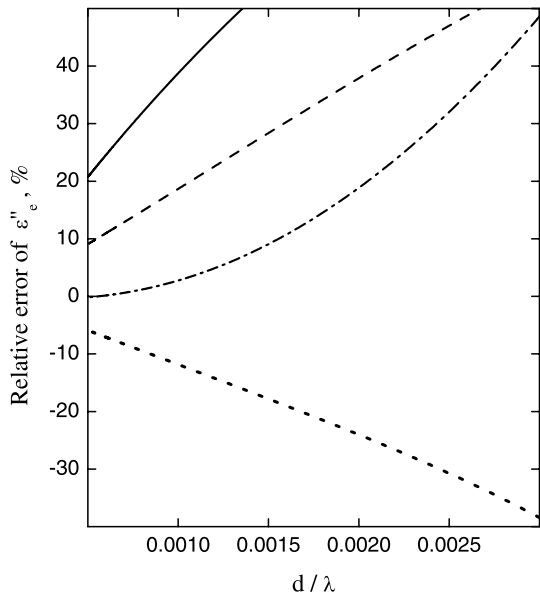

Fig. 12 Relative error of ε_e'' determined by Eq. (12) as a function of d/λ for anisotropic layers with $n_o = 2.7 + i\ 1.4$ and $n_e = 1.5 + i\ 0.3$ (solid curve), $1.5 + i\ 0.6$ (dashed curve), $1.5 + i\ 1.2$ (dotted curve), and $2.0 + i\ 1.2$ (dash-dotted curve) at $n_s^{(1)} = 1.5$, $n_s^{(2)} = 2.0$, $\varphi_a = 70°$, and $v_\Delta = v_\psi = 0$

But here we have to keep in mind that, although, on the one hand, the presumption $n_o \approx n$ is indeed justified, since the anisotropic effect is small and the values of the ellipsometric angles of anisotropic graphene are mainly determined by the ordinary refractive index n_o, on the other hand, however, the refractive index n values given in the literature are quite different, depending on the particular object to be measured.

The following problems can significantly affect the accuracy of ellipsometric measurements (regardless of which model—isotropic or anisotropic—we use in interpreting the results). First, it is clear that the diameter of the measured graphene flake must be larger than the diameter of the light spot. This is a problem in the case of graphene obtained from micromechanical cleavage of graphite since such a method makes it difficult to obtain sufficiently large graphene flakes. To a certain extent helps strong focusing of light, but this can lead to a noticeable increase in noise levels (Kravets et al. 2010) and a reduction in the accuracy of ellipsometric measurements. Note that if the area below the light spot also contains voids, then a certain averaged (effective) refractive index is measured, the value of which may be substantially lower than that of the continuous graphene layer. This value can be estimated on the basis of an effective medium approximation (EMA) theory (Humlicek 2013). For example, if there is 80% graphene in the area under the light spot and 20% voids, then according to the Bruggeman formula (Aspnes et al. 1979), we get $n = 2.35 + i\,1.14$, and if the graphene is only 50%, then $n = 1.79 + i\,0.628$ (assuming that the refractive index of the continuous graphene layer $n = 2.7 + i\,1.4$). But it should be borne in mind that strictly speaking, the EMA method applies if the characteristic size of the homogeneous regions is much smaller than the wavelength of radiation, i.e., in the case of visible light, the graphene flakes and voids should have a diameter $\leq 1\ \mu m$.

Further, sufficiently large graphene sheets can be prepared by another, widely used CVD method (Nelson et al. 2010). However, the problem here is that the number of graphene layers throughout the entire sheet is often not stable, it can change. But it is worth noting that an area with an unchanged number of layers (e.g., a monolayer) can be found by Raman spectroscopy, which relatively easily makes it possible to distinguish monolayer from a few-layer graphene. Of course, the contaminating layers on the surface of graphene or between the graphene and the substrate also have a significant effect on the measurements, but their effect will be analyzed in more detail below.

Therefore, it is advisable to pre-determine the value of n on the basis of the isotropic model, compare the obtained result with literature data, and only then use it in Eq. (8) for parameter n_o. Note that in the following computer simulation to evaluate the accuracy of formula (8) it is assumed that n_o is a known parameter whose approximate values $n_o \approx n$ are taken from the literature (Cheon et al. 2014).

In order to determine the error of Eq. (8), we give certain values for ordinary and extraordinary dielectric constants $\varepsilon_o = \varepsilon_o' + i\varepsilon_o''$ and $\varepsilon_e = \varepsilon_e'$, for thickness d, and for incident angle φ_a. Then we calculate by rigorous electromagnetic theory the exact values of $\delta\Delta$ for these given values of parameters. Next we use this calculated $\delta\Delta$ value as a "measured" quantity in the form of $\delta\Delta\,(1 - v_\Delta)$ (v_Δ represent the relative "instrumental" error of $\delta\Delta$) in Eq. (8) for calculating the approximate value $\varepsilon_e'^{(ap)}$ ($n_e'^{(ap)}$) for the unknown extraordinary dielectric constant (refractive index). The relative error of Eq. (8) can then be determined by the formula: $(\varepsilon_e' - \varepsilon_e'^{(ap)})/\varepsilon_e'$ or $n_e' - n_e'^{(ap)})/n_e'$.

Calculations show (Fig. 8) that for monographene the error of the extraordinary refractive index n_e' calculated by Eq. (8) is basically determined by an instrumental error which plays a decisive role when the thickness d is very small and the error of the approximate Eq. (8) itself is virtually irrelevant.

In general, however, the possibilities for determining all four dielectric constants ε_o', ε_o'', ε_e', and ε_e' are of greater interest. It is clear that by measuring only single wavelength ellipsometric parameters ($\delta\Psi$ and $\delta\Delta$) for one particular structure, four unknown (ε_o', ε_o'', ε_e', and ε_e'') cannot be determined because from Eqs. (1) and (2) it follows directly that the

change in the angle of incidence does not give anything because the measurements made under different angles are not independent values.

On the other hand, given the fact that it is relatively easy to transfer the graphene to various dielectric materials, it is worth analyzing the determination of anisotropic dielectric constants by a method in which measurements are made for two different structures where the 2D material is the same, but the substrate is different. Using Eqs. (1) and (2), one can obtain the following relationships:

$$\varepsilon'_o = \varepsilon_a + \frac{P^{(1)}_\Delta \varepsilon^{(2)}_s - P^{(2)}_\Delta \varepsilon^{(1)}_s}{\varepsilon^{(2)}_s - \varepsilon^{(1)}_s}, \tag{9}$$

$$\varepsilon''_o = \frac{P^{(1)}_\Psi \varepsilon^{(2)}_s - P^{(2)}_\Psi \varepsilon^{(1)}_s}{\varepsilon^{(1)}_s - \varepsilon^{(2)}_s}, \tag{10}$$

$$\varepsilon'_e = \frac{\varepsilon'_{en}}{(\varepsilon'_{en})^2 + (\varepsilon''_{en})^2}, \tag{11}$$

$$\varepsilon''_e = \frac{\varepsilon''_{en}}{(\varepsilon'_{en})^2 + (\varepsilon''_{en})^2}, \tag{12}$$

$$\varepsilon'_{en} = \frac{\varepsilon'_e}{|\varepsilon_e|^2} = \frac{1}{\varepsilon_a}\left(1 + \frac{P^{(1)}_\Delta - P^{(2)}_\Delta}{\varepsilon^{(1)}_s - \varepsilon^{(2)}_s}\right), \tag{13}$$

$$\varepsilon''_{en} = \frac{\varepsilon''_e}{|\varepsilon_e|^2} = \frac{1}{\varepsilon_a}\left(\frac{P^{(1)}_\Psi - P^{(2)}_\Psi}{\varepsilon^{(1)}_s - \varepsilon^{(2)}_s}\right), \tag{14}$$

$$P^{(i)}_\Delta = \frac{\lambda}{d}\frac{(\varepsilon_a \cos^2 \varphi^{(i)}_s - \varepsilon^{(i)}_s \cos^2 \varphi^{(i)}_a)}{4\pi n_a \cos \varphi^{(i)}_a \sin^2 \varphi^{(i)}_a}\delta\Delta^{(i)}, \tag{15}$$

$$P^{(i)}_\Psi = \frac{\lambda}{d}\frac{(\varepsilon_a \cos^2 \varphi^{(i)}_s - \varepsilon^{(i)}_s \cos^2 \varphi^{(i)}_a)}{2\pi n_a \cos \varphi^{(i)}_a \sin^2 \varphi^{(i)}_a \sin 2\Psi^{(i)}_0}\delta\Psi^{(i)}, \tag{16}$$

where $i = 1$, 2-indexes of two different incident angles $\varphi^{(1)}_a$ and $\varphi^{(2)}_a$ of light beams onto two samples with the same 2D material and different substrates with dielectric constants $\varepsilon^{(1)}_s$ and $\varepsilon^{(2)}_s$, respectively; $\delta\Delta^{(1)}$, $\delta\Psi^{(1)}$ and $\delta\Delta^{(2)}$, $\delta\Psi^{(2)}$ are the ellipsometric angles of samples 1 and 2.

The accuracy of Eqs. (9)–(12) can be estimated using computer simulations as was done in determining the precision of the previous Eq. (8). For example, in the case of graphene ($\varepsilon''_e = 0$) the errors in calculations of parameters ε'_o, ε''_o, and ε'_e on the basis of

Eqs. (9)–(11), depending on the ratio d/λ, are shown in Fig. 8. It should be noted that the error of parameter ε'_e is considerably greater than the error of parameters ε'_o and ε''_o if $v_\Delta = v_\Psi = 0$, where v_Ψ is the relative "instrumental" error of $\delta\Psi$. Nevertheless, in the current region ($10^{-3} \leq d/\lambda \leq 2 \times 10^{-3}$), the method is still applicable to the determination of parameter ε'_e (error is about 15–20%).

However, in addition to the error caused by the inaccuracy of approximate formulas, there is always an instrumental error. It follows from Eq. (9) that the error of ε'_o depends only on the error of the ellipsometric angle $\delta\Delta$ (this dependence is demonstrated by Fig. 10a). The computer simulation also shows that, in determining ε'_e, the effect of the error v_Ψ in the measurement of the ellipsometric angle $\delta\Psi$ is practically absent, only an error in the measurement of the ellipsometric angle $\delta\Delta$ plays an important role (Fig. 10b).

At the same time, the accuracy of the determination of parameter ε''_o depends only on the error v_Ψ (Fig. 11), since ε''_o is determined only with the ellipsometric angle $\delta\Psi$ (Eq. (10)). This dependence is analogous to the dependence of ε'_o on the error v_Δ.

Note that the method can, in principle, evaluate the value of parameter ε''_e, but only if the absorbance of the 2D material is very high. Formula (12) loses thought (error goes great), if $n''_e/n'_e \leq 0.3$ (Fig. 12). Adding an instrumental error only makes the situation worse, so in this case the instrumental errors v_Δ and v_Ψ cannot be higher than a few percent.

Finally, we will address another important issue. Namely, when transferring graphene onto the substrate material, a contamination layer may appear on the graphene surface, or between the graphene and the substrate material. For example, very often this is due to readily adsorbed water (Kravets et al. 2010; Novoselov et al. 2004) or PMMA if we are dealing with a graphene grown by the chemical vapor deposition method (Matkovic et al. 2013). It should be noted that the effect of such contaminating dielectric layers on ellipsometric angles of isotropic graphene-like 2D materials is analyzed in Ref. (Adamson 2018). Since the effects of anisotropy are not high, the main conclusions from the isotropic model on the effect of the contaminating layers remain valid for anisotropic 2D material. The most important conclusion about the contamination layers derived from the isotropic model lies in the fact that their effect is considerably weaker on the ellipsometric angle $\delta\Psi$ than the angle $\delta\Delta$ (Adamson 2018). As the calculations show (Fig. 13), this conclusion holds true for anisotropic 2D materials as well. Indeed, if the thickness of the contamination layer (d_C) is about two nanometers or less, its effect on the angle $\delta\Psi$ is in the order of a few thousandths of a degree. At the same time, the effect of anisotropy is in the order of a few hundredths of a degree. Thus, in the case of very thin contamination layers ($d_C \leq 2\,\text{nm}$), we can, in the first approximation, ignore their effect on the ellipsometric angle $\delta\Psi$. The situation, however, is significantly different for ellipsometric angle $\delta\Delta$. Indeed, as shown in Fig. 13, the influence of the contamination layers is in the same order of magnitude as the anisotropic effect (approximately a few tenths of a degree).

Notice that the effect of the contamination layer, of course, depends on its refractive index (n_C). When $n_C \approx n_s$, of course, there is practically no effect of the contamination layer on the ellipsometric angles (Fig. 13, dotted curves). If, however, $n_C < n_s$, then, in the case of isotropic 2D material, the effect on the angle $\delta\Delta$ is maximal if $n_C = \sqrt{n_s}$ (Adamson 2018). This result may also be used in the first approximation for anisotropic materials (Fig. 13). Consequently, if we are dealing, for example, with quartz or glass substrates, the effect of the continuous PMMA layer ($n_C = 1.49$) is practically absent, but when the contamination layer contains 50% PMMA and 50% voids, then $n_C = 1.237$ (calculation is
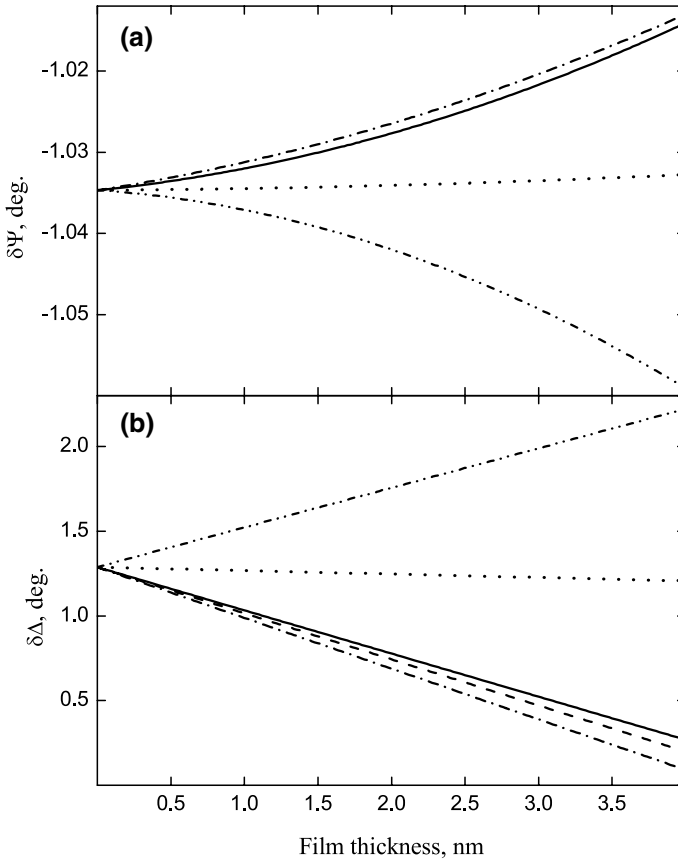
Fig. 13 Ellipsometric angles **a** $\delta\Psi$ and **b** $\delta\Delta$ as functions of thickness of dielectric contamination layers between anisotropic monographene ($n_o = 2.7 + i\ 1.4$, $n_e = 1.5$, and $d = 0.335$ nm) and substrate ($n_s = 1.5$) with different refractive indexes $n_C = 1.161$ (dashed curves), 1.237 (dash-dotted curves), 1.33 (solid curves), 1.49 (dotted curves), and 1.6 (dash-dot-dotted curves) at $\varphi_a = 70°$ and $\lambda = 500$ nm

made according to Bruggemann's formula (Aspnes et al. 1979)) and the effect of such a layer on the angle $\delta\Delta$ is already large (Fig. 13).

Therefore, in summary, it can be said that, according to the method presented in this paper, the determination of the anisotropic constants of 2D materials is possible only in the case of a very pure technological process in which the transfer of graphene to the substrates does not create contaminating layers.

4 Conclusion

An efficient approach for diagnostics of the anisotropic dielectric constants of 2D materials by ellipsometry is proposed. It is based on the analytical solution of the ellipsometric inversion problem. As a result the data handling to determine the dielectric function does not require (1) knowledge of the dispersion law for the dielectric function and (2) the use of complex numerical methods. The method allows the application of a point-by-point

technique, i.e. an independent treatment the points of the spectrum. It also makes possible to specify the unknown anisotropic constants without knowledge of their initial guesses. The method is well suited for studying the anisotropic optical properties of graphene and graphene-like 2D materials. But this method also offers an interest in 2D materials whose optical properties have complexity and which cannot be described by standard dielectric function models as various nanoparticle films.

References

Adamson, P.: Inverse relationships for reflection diagnostics of uniaxially anisotropic nanoscale films on isotropic materials. Appl. Opt. **50**, 2773–2783 (2011)

Adamson, P.: Reflectance calculations of anisotropic dielectric constants of graphene-like two-dimensional materials. Appl. Opt. **56**, 7832–7840 (2017)

Adamson, P.: A method for reducing the effect of surface contamination layers in reflection diagnostics of graphene-like 2D materials. NANO **13**, 1850044 (2018)

Aspnes, D.E., Theeten, J.B., Hottier, F.: Investigation of effective-medium models of microscopic surface roughness by spectroscopic ellipsometry. Phys. Rev. B **20**, 3292–3302 (1979)

Azzam, R.M.A., Bashara, N.M.: Ellipsometry and Polarized Light. North-Holland, Amsterdam (1977)

Battie, Y., Izquierdo-Lorenzo, I., Resano-Garcia, A., En, Naciri A., Akil, S., Adam, P.M., Jradi, S.: How to determine the morphology of plasmonic nanocrystals without transmission electron microscopy? J. Nanopart. Res. **18**, 217 (2016)

Battie, Y., Izquierdo-Lorenzo, I., Resano-Garcia, A., En, Naciri A., Akil, S., Adam, P.M., Jradi, S.: Determination of gold nanoparticle shape from absorption spectroscopy and ellipsometry. Appl. Surf. Sci. **421**, 301–309 (2017)

Bedeaux, D., Vlieger, J.: Optical Properties of Surfaces. Imperial College Press, London (2001)

Cheon, S., Kihm, K.D., Kim, H., Lim, G., Park, J.S., Lee, J.S.: How to reliably determine the complex refractive index of graphene by using two independent measurement constraints. Sci. Reports **4**, 6364 (2014)

Duong, D.L., Yun, S.J., Lee, Y.H.: Van der Waals layered materials: opportunities and challenges. ACS Nano **11**, 11803–11830 (2017)

Ferrari, A.C.: Raman spectroscopy of graphene and graphite: disorder, electron–phonon coupling, doping and nonadiabatic effects. Solid State Commun. **143**, 47–57 (2007)

Fujiwara, H.: Spectroscopic Ellipsometry: Principles and Applications. Wiley, New York (2007)

Garcia-Caurel, E., de Martino, A., Gaston, J.P., Yan, L.: Application of spectroscopic ellipsometry and Mueller ellipsometry to optical characterization. Appl. Spectrosc. **67**, 1–21 (2013)

Gilliot, M.: Inversion of ellipsometry data using constrained spline analysis. Appl. Opt. **56**, 1173–1182 (2017)

Gwo, S., Chen, H.Y., Lin, M.H., Sun, L., Li, X.: Nanomanipulation and controlled self-assembly of metal nanoparticles and nanocrystals for plasmonics. Chem. Soc. Rev. **45**, 5672–5716 (2016)

Humlicek, J.: Data analysis for nanomaterials: effective medium approximation, its limits and implementations. In: Losurdo, M., Hingerl, K. (eds.) Ellipsometry at the Nanoscale. Springer, Berlin (2013)

Isic, G., Jakovljevic, M., Filipovic, M., Jovanovic, D., Vasic, B., Lazovic, S., Puac, N., Petrovic, Z., Kostic, R., Gajic, R., Humlicek, J., Losurdo, M., Bruno, G., Bergmair, I., Hingerl, K.: Spectroscopic ellipsometry of few-layer graphene. J. Nanophoton. **5**, 051809 (2011)

Jellison, G.E., Hunn, J.D., Lee, H.N.: Measurement of optical functions of highly oriented pyrolytic graphite in the visible. Phys. Rev. B **76**, 085125 (2007)

Klintenberg, M., Lebegue, S., Ortiz, C., Sanyal, B., Fransson, J., Eriksson, O.: Evolving properties of two-dimensional materials: from graphene to graphite. J. Phys.: Condens. Matter **21**, 335502 (2009)

Kravets, V.G., Grigorenko, A.N., Nair, R.R., Blake, P., Anissimova, S., Novoselov, K.S., Geim, A.K.: Spectroscopic ellipsometry of graphene and an exciton-shifted van Hove peak in absorption. Phys. Rev. B **81**, 155413 (2010)

Lazzari, R., Renaud, G., Revenant, C., Jupille, J., Borensztein, Y.: Adhesion of growing nanoparticles at a glance: surface differential reflectivity spectroscopy and grazing incidence small angle X-ray scattering. Phys. Rev. B **79**, 125428 (2009)

Li, W., Cheng, G., Liang, Y., Tian, B., Liang, X., Peng, L., Walker, A.R.H., Gundlach, D.J., Nguyen, N.V.: Broadband optical properties of graphene by spectroscopic ellipsometry. Carbon **99**, 348–353 (2016)

Li, X., Tao, L., Chen, Z., Fang, H., Li, X., Wang, X., Xu, J.B., Zhu, H.: Graphene and related two-dimensional materials: structure-property relationships for electronics and optoelectronics. Appl. Phys. Rev. **4**, 021306 (2017)

Losurdo, M., Bergmair, M., Bruno, G., Cattelan, D., Cobet, C., de Martino, A., Fleischer, K., Dohcevic-Mitrovic, Z., Esser, N., Galliet, M., Gajic, R., Hemzal, D., Hingerl, K., Humlicek, J., Ossikovski, R., Popovic, Z.V., Saxl, O.: Spectroscopic ellipsometry and polarimetry for materials and systems analysis at the nanometer scale: state-of-the-art, potential, and perspectives. J. Nanopart. Res. **11**, 1521–1554 (2009)

Lui, C.H., Malard, L.M., Kim, S.H., Lantz, G., Laverge, F.E., Saito, R., Heinz, T.F.: Observation of layer-breathing mode vibrations in few-layer graphene through combination Raman scattering. Nano Lett. **12**, 5539–5544 (2012)

Matkovic, A., Ralevic, U., Chhikara, M., Jakovljevic, M., Jovanovic, D., Bratina, G., Gajic, R.: Influence of transfer residue on the optical properties of chemical vapor deposited graphene investigated through spectroscopic ellipsometry. J. Appl. Phys. **114**, 093505 (2013)

Min, H., MacDonald, A.H.: Origin of universal optical conductivity and optical stacking sequence identification in multilayer graphene. Phys. Rev. Lett. **103**, 067402 (2009)

Nelson, F.J., Kamineni, V.K., Zhang, T., Comfort, E.S., Lee, J.U., Diebold, A.C.: Optical properties of large-area polycrystalline chemical vapor deposited graphene by spectroscopic ellipsometry. Appl. Phys. Lett. **97**, 253110 (2010)

Nelson, F., Sandin, A., Dougherty, D.B., Aspnes, D.E., Rowe, J.E., Diebold, A.C.: Optical and structural characterization of epitaxial graphene on vicinal 6H–SiC(0001)–Si by spectroscopic ellipsometry, Auger spectroscopy, and STM. J. Vac. Sci. Technol. B **30**, 04E106 (2012)

Novoselov, K.S., Geim, A.K., Morozov, S.V., Jiang, D., Zhang, Y., Dubonos, S.V., Grigorieva, I.V., Firsov, A.A.: Electric field effect in atomically thin carbon films. Science **306**, 666–669 (2004)

Novoselov, K.S., Falko, V.I., Colombo, L., Gellert, P.R., Schwab, M.G., Kim, K.: A roadmap for graphene. Nature **490**, 192–200 (2012)

Oates, T.W.H., Wormeester, H., Arwin, H.: Characterization of plasmonic effects in thin films and metamaterials using spectroscopic ellipsometry. Prog. Surf. Sci. **86**, 328–376 (2011a)

Oates, T.W.H., Ranjan, M., Facsko, S., Arwin, H.: Highly anisotropic effective dielectric functions of silver nanoparticle arrays. Opt. Express **19**, 2014–2028 (2011b)

Ochoa-Martínez, E., Gabás, M., Barrutia, L., Pesquera, A., Centeno, A., Palanco, S., Zurutuza, A., Algora, C.: Determination of a refractive index and an extinction coefficient of standard production of CVD-graphene. Nanoscale **7**, 1491–1500 (2015)

Shearer, C.J., Slattery, A.D., Stapleton, A.J., Shapter, J.G., Gibson, C.T.: Accurate thickness measurement of graphene. Nanotechnology **27**, 125704 (2016)

Song, B., Gu, H., Zhu, S., Jiang, H., Chen, X., Zhang, C., Liu, S.: Broadband optical properties of graphene and HOPG investigated by spectroscopic Mueller matrix ellipsometry. Appl. Surf. Sci. **439**, 1079–1087 (2018)

Tan, P.H., Han, W.P., Zhao, W.J., Wu, Z.H., Chang, K., Wang, H., Wang, Y.F., Bonini, N., Marzari, N., Pugno, N., Savini, G., Lombardo, A., Ferrari, A.C.: The shear mode of multilayer graphene. Nat. Mater. **11**, 294–300 (2012)

Tompkins, H.G., Irene, E.A.: Handbook of Ellipsometry. William Andrew Publishing, Norwich (2005)

Toudert, J., Simonot, L., Camelio, S., Babonneau, D.: Advanced optical effective medium modeling for a single layer of polydisperse ellipsoidal nanoparticles embedded in a homogeneous dielectric medium: surface plasmon resonances. Phys. Rev. B **86**, 045415 (2012)

Wang, Y.Y., Gao, R.X., Ni, Z.H., He, H., Guo, S.P., Yang, H.P., Cong, C.X., Yu, T.: Thickness identification of two-dimensional materials by optical imaging. Nanotechnology **23**, 495713 (2012)

Weber, J.W., Calado, V.E., van de Sanden, M.C.M.: Optical constants of graphene measured by spectroscopic ellipsometry. Appl. Phys. Lett. **97**, 091904 (2010)

Wurstbauer, Ul, Röling, C., Wurstbauer, Ur, Wegscheider, W., Vaupe, M., Thiesen, P.H., Weiss, D.: Imaging ellipsometry of graphene. Appl. Phys. Lett. **97**, 231901 (2010)

Yeh, P.: Optical Waves in Layered Media. Wiley, New York (2005)

Zaglmayr, H., Hu, C.G., Sun, L.D., Zeppenfeld, P.: Optical referencing in differential reflectance spectroscopy. Meas. Sci. Technol. **25**, 115603 (2014)